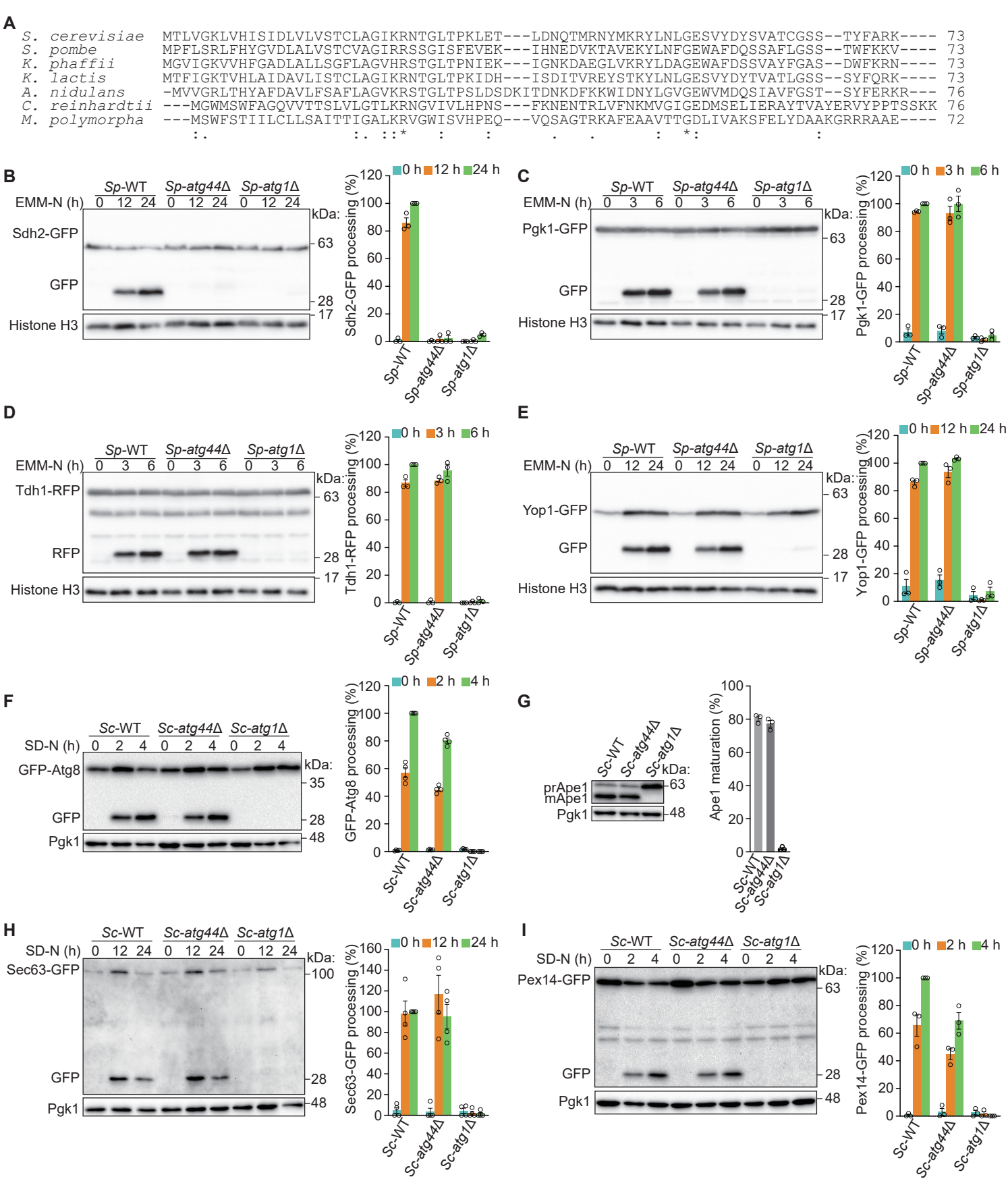
A
S. cerevisiae MTLVGKLVHISIDLVLVSTCLAGIKRNTGLTPKLET---LDNQTMRNYMKRYLNLGESVYDYSVATCGSS--TYFARK---- 73
S. pombe MPFLSRLFHYGVDLALVSTCVAGIRRSSGISFEVEK---IHNEDVKTAVEKYLNFGEWAFDQSSAFLGSS--TWFKKV---- 73
K. phaffii MGVIGKVVHFGADLALLSGFLAGVHRSTGLTPNIEK---IGNKDAEGLVKRYLDAGEWAFDSSVAYFGAS--DWFKRN---- 73
K. lactis MTFIGKTVHLAIDAVLISTCLAGIKRNTGLTPKIDH---ISDITVREYSTKYLNLGESVYDYTVATLGSS--SYFQRK---- 73
A. nidulans -MVVGRLTHYAFDAVLFSAFLAGVKRSTGLTPSLDSDKITDNKDFKKWIDNYLGVGEWVMDQSIAVFGST--SYFERKR--- 76
C. reinhardtii ---MGWMSWFAGQVVTTSLVLGTLKRNGVIVLHPNS---FKNENTRLVFNKMVGIGEDMSELIERAYTVAYERVYPPTSSKK 76
M. polymorpha ---MSWFSTIILCLLSAITTIGALKRVGWISVHPEQ---VQSAGTRKAFEAAVTTGDLIVAKSFELYDAAKGRRRAAE---- 72
B
Sp-WT
Sp-atg44Δ
Sp-atg1Δ
EMM-N (h)
0 12 24 0 12 24 0 12 24
kDa:
Sdh2-GFP
GFP
Histone H3
63
28
17
0 h 12 h 24 h
Sdh2-GFP processing (%)
Sp-WT
Sp-atg44Δ
Sp-atg1Δ
C
Sp-WT
Sp-atg44Δ
Sp-atg1Δ
EMM-N (h)
0 3 6 0 3 6 0 3 6
kDa:
Pgk1-GFP
GFP
Histone H3
63
28
17
0 h 3 h 6 h
Pgk1-GFP processing (%)
Sp-WT
Sp-atg44Δ
Sp-atg1Δ
D
Sp-WT
Sp-atg44Δ
Sp-atg1Δ
EMM-N (h)
0 3 6 0 3 6 0 3 6
kDa:
Tdh1-RFP
RFP
Histone H3
63
28
17
0 h 3 h 6 h
Tdh1-RFP processing (%)
Sp-WT
Sp-atg44Δ
Sp-atg1Δ
E
Sp-WT
Sp-atg44Δ
Sp-atg1Δ
EMM-N (h)
0 12 24 0 12 24 0 12 24
kDa:
Yop1-GFP
GFP
Histone H3
63
28
17
0 h 12 h 24 h
Yop1-GFP processing (%)
Sp-WT
Sp-atg44Δ
Sp-atg1Δ
F
Sc-WT
Sc-atg44Δ
Sc-atg1Δ
SD-N (h)
0 2 4 0 2 4 0 2 4
kDa:
GFP-Atg8
GFP
Pgk1
35
28
48
0 h 2 h 4 h
GFP-Atg8 processing (%)
Sc-WT
Sc-atg44Δ
Sc-atg1Δ
G
Sc-WT
Sc-atg44Δ
Sc-atg1Δ
kDa:
prApe1
mApe1
Pgk1
63
48
Ape1 maturation (%)
Sc-WT
Sc-atg44Δ
Sc-atg1Δ
H
Sc-WT
Sc-atg44Δ
Sc-atg1Δ
SD-N (h)
0 12 24 0 12 24 0 12 24
kDa:
Sec63-GFP
GFP
Pgk1
100
28
48
0 h 12 h 24 h
Sec63-GFP processing (%)
Sc-WT
Sc-atg44Δ
Sc-atg1Δ
I
Sc-WT
Sc-atg44Δ
Sc-atg1Δ
SD-N (h)
0 2 4 0 2 4 0 2 4
kDa:
Pex14-GFP
GFP
Pgk1
63
28
48
0 h 2 h 4 h
Pex14-GFP processing (%)
Sc-WT
Sc-atg44Δ
Sc-atg1Δ
J
Sc-atg44Δ
CUP1-
empty
ATG44
ATG44 -FLAG
SD-N (h)
0 6 0 6 0 6
kDa:
Idh1-GFP
GFP
Sc-Atg44
Pgk1
63
28
8.7
48
K
Na2CO3
Mito
Sup
Pellet
kDa:
Atg33
Cox2
Atp2
Sc-Atg44
17
48
8.7
L
Non-treated
ProK
Hypo + ProK
TritonX + ProK
kDa:
Sc-Atg44-FLAG
Atg33
Mia40-GFP
Atp2
8.7
17
48
M
Non-treated
ProK
Hypo + ProK
TritonX + ProK
kDa:
Sp-Atg44
Tom70-GFP
Mic60-FLAG
Tuf1-RFP
100
75
63

**Figure S1. Atg44 is specifically required for mitophagy, related to Figure 1**

(A) Protein sequence alignment of Atg44-like proteins from different species. *S. cerevisiae*, *Saccharomyces cerevisiae*; *S. pombe*, *Schizosaccharomyces pombe*; *K. phaffii*, *Komagataella phaffii/Pichia pastoris*; *K. lactis*, *Kluyveromyces lactis*; *A. nidulans*, *Aspergillus nidulans*; *C. reinhardtii*, *Chlamydomonas reinhardtii*; *M. polymorpha*, *Marchantia polymorpha*. Asterisk, fully conserved residue; colon, conservation between groups of strongly similar properties; period, conservation between groups of weakly similar properties.

(B–E) The indicated *S. pombe* strains expressing Sdh2-GFP, Pgk1-GFP, Tdh1-RFP, or Yop1-GFP were grown in EMM and shifted to EMM-N. Cells were collected at the indicated time points and Sdh2-GFP, Pgk1-GFP, Tdh1-RFP, or Yop1-GFP processing was monitored by immunoblotting to observe mitophagy (B), macroautophagy (C, D), and reticulophagy (E).

(F, H, and I) The indicated *S. cerevisiae* strains expressing GFP-Atg8, Sec63-GFP, or Pex14-GFP were grown in YPD (F, H) or YTO (I) and shifted to SD-N. Cells were collected at the indicated time and GFP-Atg8, Sec63-GFP, or Pex14-GFP processing was monitored by immunoblotting to observe macroautophagy (F), reticulophagy (H), and pexophagy (I).

(G) The indicated *S. cerevisiae* strains were grown in YPD until the early log growth phase. Cells were collected and analyzed by immunoblotting using an anti-Ape1 antibody. The positions of precursor and mature Ape1 are indicated.

The results represent the mean and SD of three (B–E, G, and I) or four (F and H) experiments.

(J) Mitophagy in *S. cerevisiae atg44*Δ cells exogenously expressing *Sc-ATG44* or *Sc-ATG44*-FLAG under the *CUP1* promoter was monitored by the Idh1-GFP processing assay as shown in Figure 1C.

(K) Isolated mitochondria (Mito) from *S. cerevisiae* cells were treated with 0.1 M sodium carbonate (pH 11.0) and separated into pellet and supernatant fractions by ultracentrifugation. Samples were TCA precipitated and subjected to immunoblotting.

(L and M) Isolated mitochondria from *S. cerevisiae* cells expressing *Sc*-Atg44-FLAG and Mia40-GFP or *S. pombe* expressing Tom70-GFP, Mic60-FLAG, and Tuf1-RFP were treated with ProK with or without hypotonic treatment or Triton X-100 (TritonX). Samples were TCA precipitated and subjected to immunoblotting.

Histone H3 (B–E) and Pgk1 (F–I, and J) were used as loading controls.

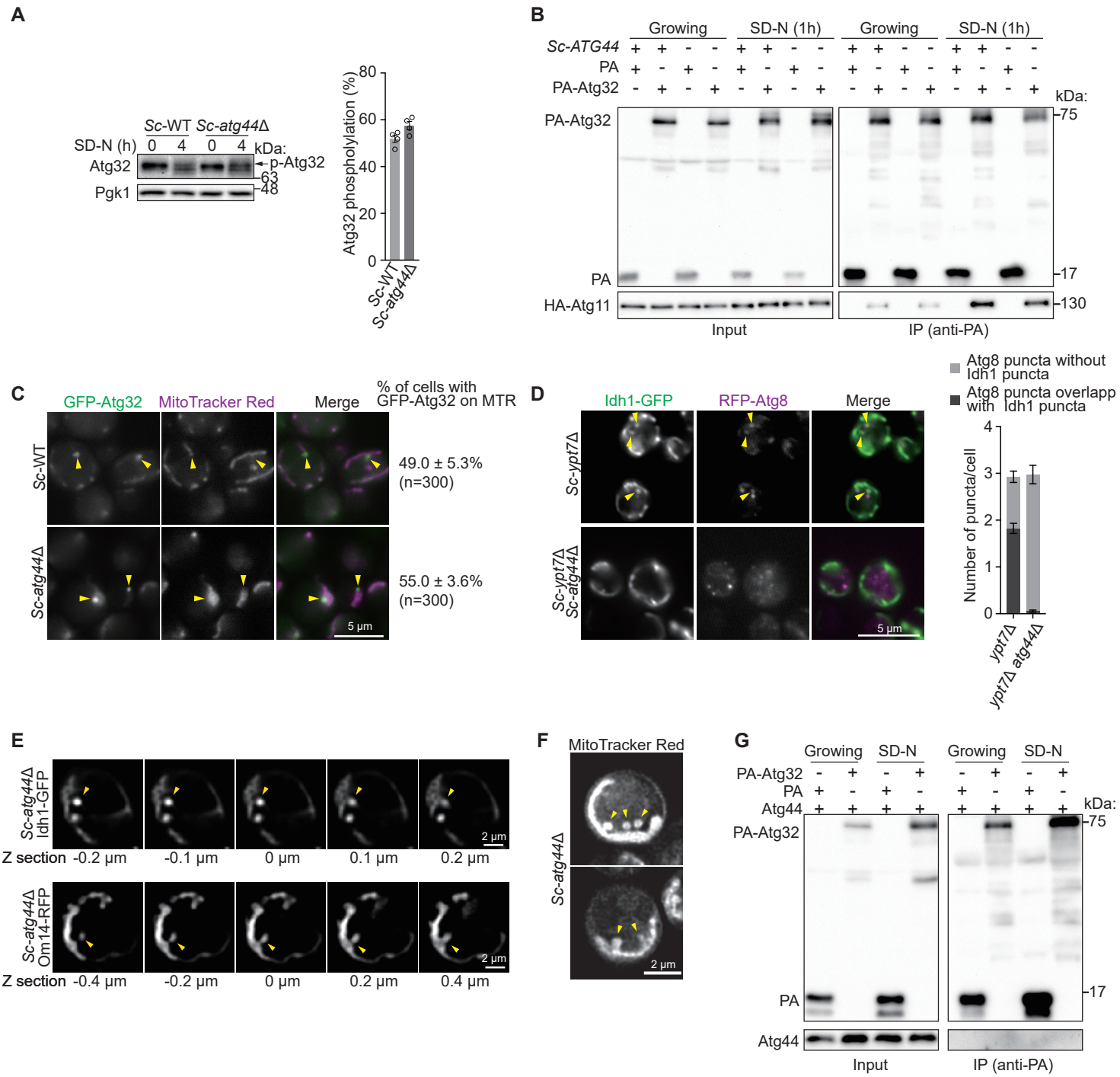
A
Sc-WT Sc-atg44Δ
SD-N (h) 0 4 0 4 kDa:
Atg32
p-Atg32
63
Pgk1
48
Atg32 phosphorylation (%)
80
60
40
20
0
Sc-WT
Sc-atg44Δ
B
Growing
SD-N (1h)
Growing
SD-N (1h)
Sc-ATG44
PA
PA-Atg32
kDa:
75
PA-Atg32
PA
17
HA-Atg11
130
Input
IP (anti-PA)
C
GFP-Atg32
MitoTracker Red
Merge
% of cells with GFP-Atg32 on MTR
Sc-WT
49.0 ± 5.3% (n=300)
Sc-atg44Δ
55.0 ± 3.6% (n=300)
5 µm
D
Idh1-GFP
RFP-Atg8
Merge
Sc-ypt7Δ
Sc-ypt7Δ Sc-atg44Δ
5 µm
Atg8 puncta without Idh1 puncta
Atg8 puncta overlapp with Idh1 puncta
Number of puncta/cell
4
3
2
1
0
ypt7Δ
ypt7Δ atg44Δ
E
Sc-atg44Δ Idh1-GFP
2 µm
Z section -0.2 µm -0.1 µm 0 µm 0.1 µm 0.2 µm
Sc-atg44Δ Om14-RFP
2 µm
Z section -0.4 µm -0.2 µm 0 µm 0.2 µm 0.4 µm
F
MitoTracker Red
Sc-atg44Δ
2 µm
G
Growing
SD-N
Growing
SD-N
PA-Atg32
PA
Atg44
kDa:
75
PA-Atg32
PA
17
Atg44
Input
IP (anti-PA)

**Figure S2. Atg44 is required for mitophagosome formation, but not for Atg32 phosphorylation and Atg32-Atg11 interaction, related to Figure 2**

(A) The indicated *S. cerevisiae* strains were cultured in YPL medium until mid-log growth phase and shifted to SD-N for 4 h. The phosphorylation status of Atg32 was analyzed by immunoblotting using an anti-Atg32 antibody. The position of phosphorylated Atg32 was indicated. Pgk1 was used as a loading control. The ratio of phosphorylated Atg32 per total Atg32 was quantified. The results represent the mean and SD of four experiments.

(B) *S. cerevisiae* strains expressing HA-Atg11 and PA only or PA-Atg32 were cultured in SMD until early log growth phase and shifted to SD-N medium for 1 h. PA or PA-Atg32 was precipitated using immunoglobulin G (IgG)-Sepharose from cell lysates. Immunoblots of total cell lysates (input) and the IgG precipitates (IP) were probed with anti-PA and anti-HA antibodies.

(C) The indicated *S. cerevisiae* cells expressing GFP-Atg32 were grown in YPD and shifted to SD-N for 1 h in the presence of MitoTracker Red CMXRos for 30 min and analyzed by fluorescence microscopy. Arrowheads indicate accumulation of GFP-Atg32 on mitochondria. The percentage of cells showing GFP-Atg32 accumulation on the mitochondria was quantified. The results represent the mean and SD of three experiments. The value of n represents the number of observed cells.

(D) The indicated *S. cerevisiae* cells expressing Idh1-GFP and RFP-Atg8 were grown in SML and shifted to SD-N medium for 6 h and then analyzed by fluorescence microscopy. Arrowheads indicate presumed mitophagosomes. The results represent the mean and SD of the number of RFP-Atg8 puncta that colocalized with or without Idh1-GFP puncta per cell. 176 *Sc-ypt7*Δ cells and 122 *Sc-ypt7*Δ *Sc-atg44*Δ cells were analyzed.

(E) *S. cerevisiae atg44*Δ cells expressing Idh1-GFP or Om14-RFP were grown in YPL and shifted to SD-N medium for 6 h and then analyzed by fluorescence microscopy. A 3D-deconvoluted series of Z-axis section images is shown. The punctate image of Idh1-GFP or Om14-RFP at a single Z-section connected with the main body of mitochondria in different Z-sections (arrowheads). Scale bars and their lengths are provided in each panel.

(F) *S. cerevisiae atg44*Δ cells were grown in YPL and shifted to SD-N medium for 6 h and then analyzed by super-resolution microscopy. Cells were stained with MitoTracker Red CMXRos for 1 h. Deconvolution images are shown.

(G) *S. cerevisiae* cells expressing Atg44 and protein A (PA) or PA-Atg32 were cultured in SMD medium until the early log growth phase and shifted to SD-N medium for 1 h. PA or PA-Atg32 was precipitated using immunoglobulin G (IgG)-Sepharose from cell lysates. Immunoblots of total cell lysates (input) and the IgG precipitates (IP) were probed with anti-PA and anti-Atg44 antibodies.

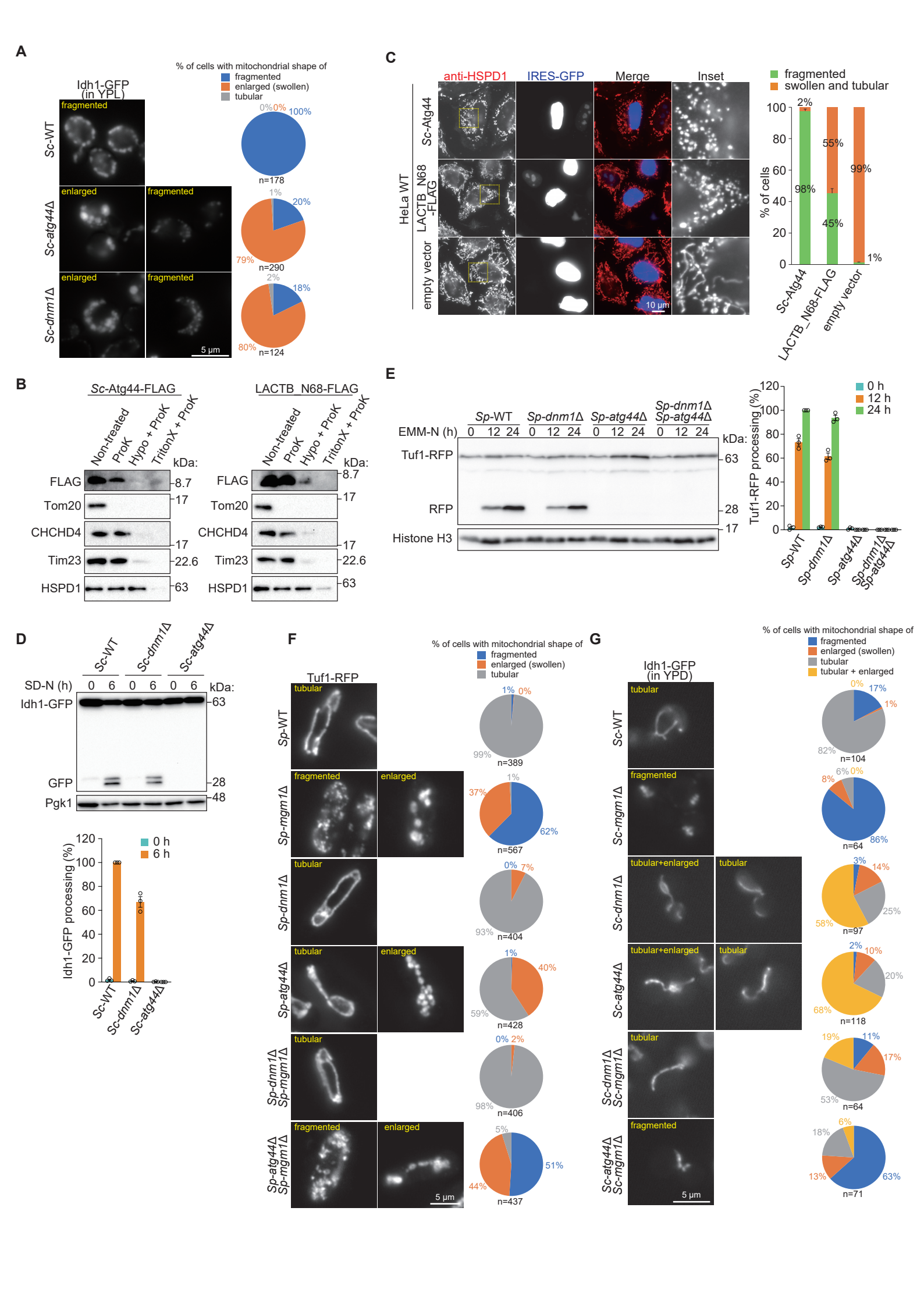
A
Idh1-GFP (in YPL)
% of cells with mitochondrial shape of
fragmented
enlarged (swollen)
tubular
Sc-WT
Sc-atg44Δ
Sc-dnm1Δ
fragmented
enlarged
5 μm
0% 0% 100%
n=178
1% 20% 79%
n=290
2% 18% 80%
n=124
B
Sc-Atg44-FLAG
LACTB_N68-FLAG
Non-treated
ProK
Hypo + ProK
TritonX + ProK
kDa:
FLAG
Tom20
CHCHD4
Tim23
HSPD1
8.7
17
17
22.6
63
C
anti-HSPD1
IRES-GFP
Merge
Inset
HeLa WT
Sc-Atg44
LACTB_N68-FLAG
empty vector
10 μm
fragmented
swollen and tubular
% of cells
2%
98%
55%
45%
99%
1%
Sc-Atg44
LACTB_N68-FLAG
empty vector
D
Sc-WT
Sc-dnm1Δ
Sc-atg44Δ
SD-N (h)
0 6 0 6 0 6
kDa:
Idh1-GFP
GFP
Pgk1
63
28
48
Idh1-GFP processing (%)
0 h
6 h
E
Sp-WT
Sp-dnm1Δ
Sp-atg44Δ
Sp-dnm1Δ Sp-atg44Δ
EMM-N (h)
0 12 24 0 12 24 0 12 24 0 12 24
kDa:
Tuf1-RFP
RFP
Histone H3
63
28
17
Tuf1-RFP processing (%)
0 h
12 h
24 h
Sp-WT
Sp-dnm1Δ
Sp-atg44Δ
Sp-dnm1Δ Sp-atg44Δ
F
Tuf1-RFP
% of cells with mitochondrial shape of
fragmented
enlarged (swollen)
tubular
Sp-WT
Sp-mgm1Δ
Sp-dnm1Δ
Sp-atg44Δ
Sp-dnm1Δ Sp-mgm1Δ
Sp-atg44Δ Sp-mgm1Δ
tubular
fragmented
enlarged
5 μm
1% 0% 99%
n=389
1% 37% 62%
n=567
0% 7% 93%
n=404
1% 40% 59%
n=428
0% 2% 98%
n=406
5% 44% 51%
n=437
G
Idh1-GFP (in YPD)
% of cells with mitochondrial shape of
fragmented
enlarged (swollen)
tubular
tubular + enlarged
Sc-WT
Sc-mgm1Δ
Sc-dnm1Δ
Sc-atg44Δ
Sc-dnm1Δ Sc-mgm1Δ
Sc-atg44Δ Sc-mgm1Δ
tubular
fragmented
tubular+enlarged
5 μm
0% 17% 1% 82%
n=104
6% 0% 8% 86%
n=64
3% 14% 58% 25%
n=97
2% 10% 68% 20%
n=118
19% 11% 17% 53%
n=64
6% 18% 13% 63%
n=71

**Figure S3. Atg44 and Dnm1 have different roles in mitochondrial fission, related to Figures 3 and 4**

(A) *S. cerevisiae* cells expressing Idh1-GFP were grown in YPL and analyzed by fluorescence microscopy. Cells were classified according to their mitochondrial morphology (fragmented, enlarged, tubular in shape), and their ratio was quantified.

(B) Isolated mitochondria from HeLa cells expressing *Sc*-Atg44-FLAG or LACTB_N68-FLAG were treated with ProK with or without hypotonic treatment (Hypo) or Triton X-100 (TritonX). Samples were TCA precipitated and subjected to immunoblotting with anti-FLAG, anti-Tom20 (OMM), anti-CHCHD4 (IMS), anti-Tim23 (IMM), and anti-HSPD1 (matrix) antibodies.

(C) Wild-type HeLa cells were transfected with the *Sc*-Atg44 or LACTB_N68-FLAG expression IRES-GFP-NLS vectors and the mitochondrial morphology was analyzed by immunofluorescence microscopy using an anti-HSPD1/HSP60 antibody. Nuclear GFP-expressing cells were classified according to whether their mitochondria were fragmented or swollen/tubular in shape, and their ratio was quantified. The results represent the mean and SD of three experiments. More than 60 cells were analyzed for each experiment.

(D and E) Mitophagy in the indicated *S. cerevisiae* (D) or *S. pombe* (E) strains was monitored by the Idh1-GFP or Tuf1-RFP processing assay as shown in Figure 1C or 1A, respectively.

(F and G) The indicated *S. pombe* (F) or *S. cerevisiae* (G) cells expressing Tuf1-RFP or Idh1-GFP were grown in EMM or YPD, respectively, and analyzed by fluorescence microscopy. Cells were classified according to their mitochondrial morphology (fragmented, enlarged, tubular, or a mixture of tubular and enlarged in shape), and their ratio was quantified.

The value of n represents the number of observed cells. Scale bars and their lengths are provided in each panel.

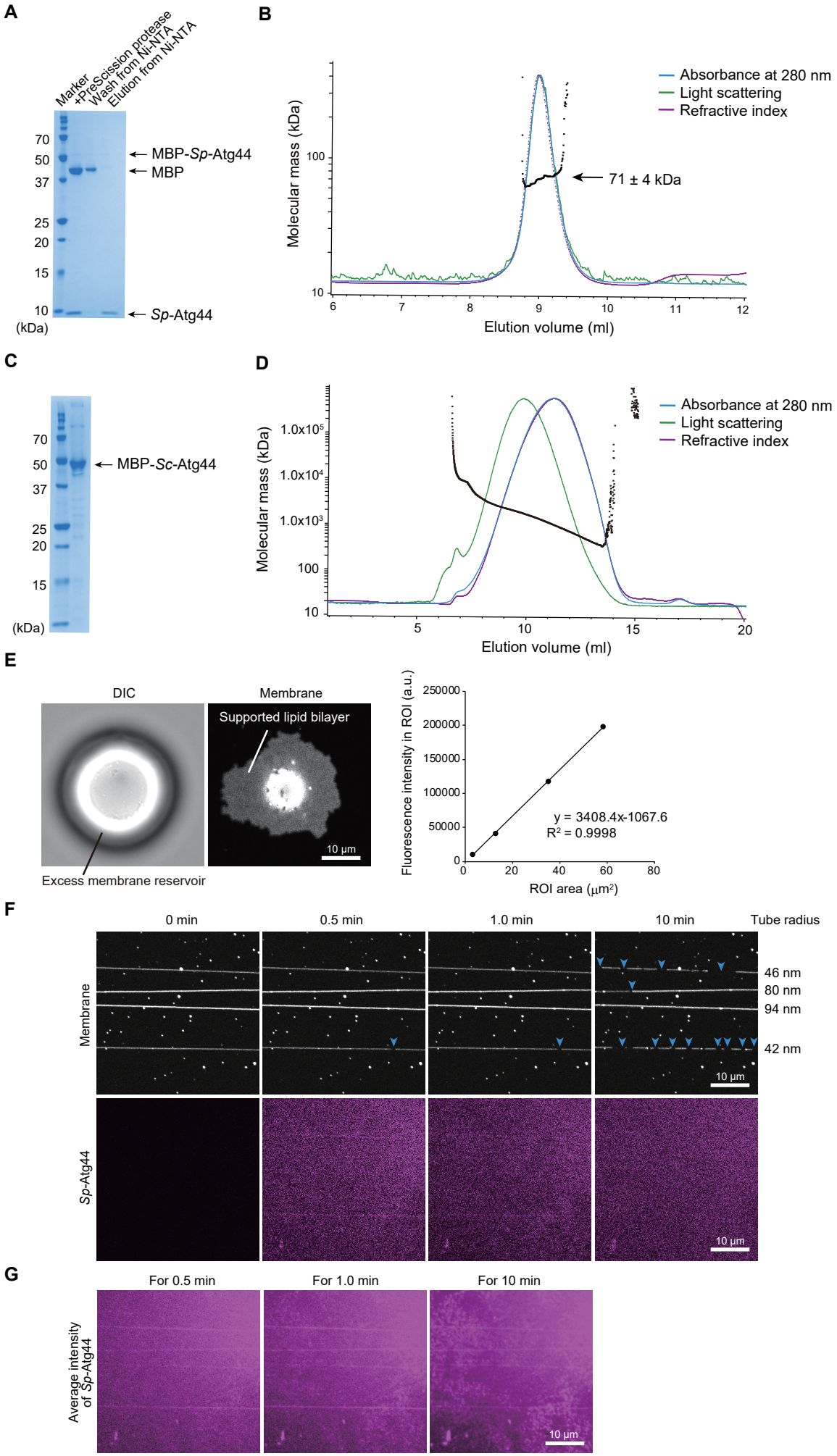
A
Marker
+PreScission protease
Wash from Ni-NTA
Elution from Ni-NTA
70
50
37
25
20
15
10
(kDa)
MBP-Sp-Atg44
MBP
Sp-Atg44
B
Absorbance at 280 nm
Light scattering
Refractive index
Molecular mass (kDa)
100
10
71 ± 4 kDa
6
7
8
9
10
11
12
Elution volume (ml)
C
70
50
37
25
20
15
(kDa)
MBP-Sc-Atg44
D
Absorbance at 280 nm
Light scattering
Refractive index
Molecular mass (kDa)
1.0x10^5
1.0x10^4
1.0x10^3
100
10
5
10
15
20
Elution volume (ml)
E
DIC
Membrane
Supported lipid bilayer
10 μm
Excess membrane reservoir
Fluorescence intensity in ROI (a.u.)
250000
200000
150000
100000
50000
0
y = 3408.4x-1067.6
R² = 0.9998
0
20
40
60
80
ROI area (μm²)
F
0 min
0.5 min
1.0 min
10 min
Tube radius
Membrane
46 nm
80 nm
94 nm
42 nm
10 μm
Sp-Atg44
10 μm
G
For 0.5 min
For 1.0 min
For 10 min
Average intensity of Sp-Atg44
10 μm

**Figure S4. Recombinant Atg44 mediates fission of lipid nanotubes, related to Figure 5**

(A and B) SDS-PAGE (A) and SEC-MALS (B) analyses of prepared *Sp*-Atg44.

(C and D) SDS-PAGE (C) and SEC-MALS (D) analyses of MBP-*Sc*-Atg44.

(E) Correlation factor between fluorescence intensity in the region of interest (ROI) and ROI area. Liss Rhod PE in the membrane was observed. The fluorescence intensity of the supported lipid bilayer spilled out from excess membrane reservoir was measured and plotted against ROI area to calculate the correlation factor for the estimation of tube radius. a.u., arbitrary units.

(F) Confocal imaging of tube fission by *Sp*-Atg44. AF647-*Sp*-Atg44 and liss Rhod PE in lipid nanotubes were observed. Fission parts are labeled by blue arrowheads.

(G) Time-averaged fluorescence intensity of AF647-*Sp*-Atg44 on lipid nanotubes in (F).

Scale bars and their lengths are provided in each panel.

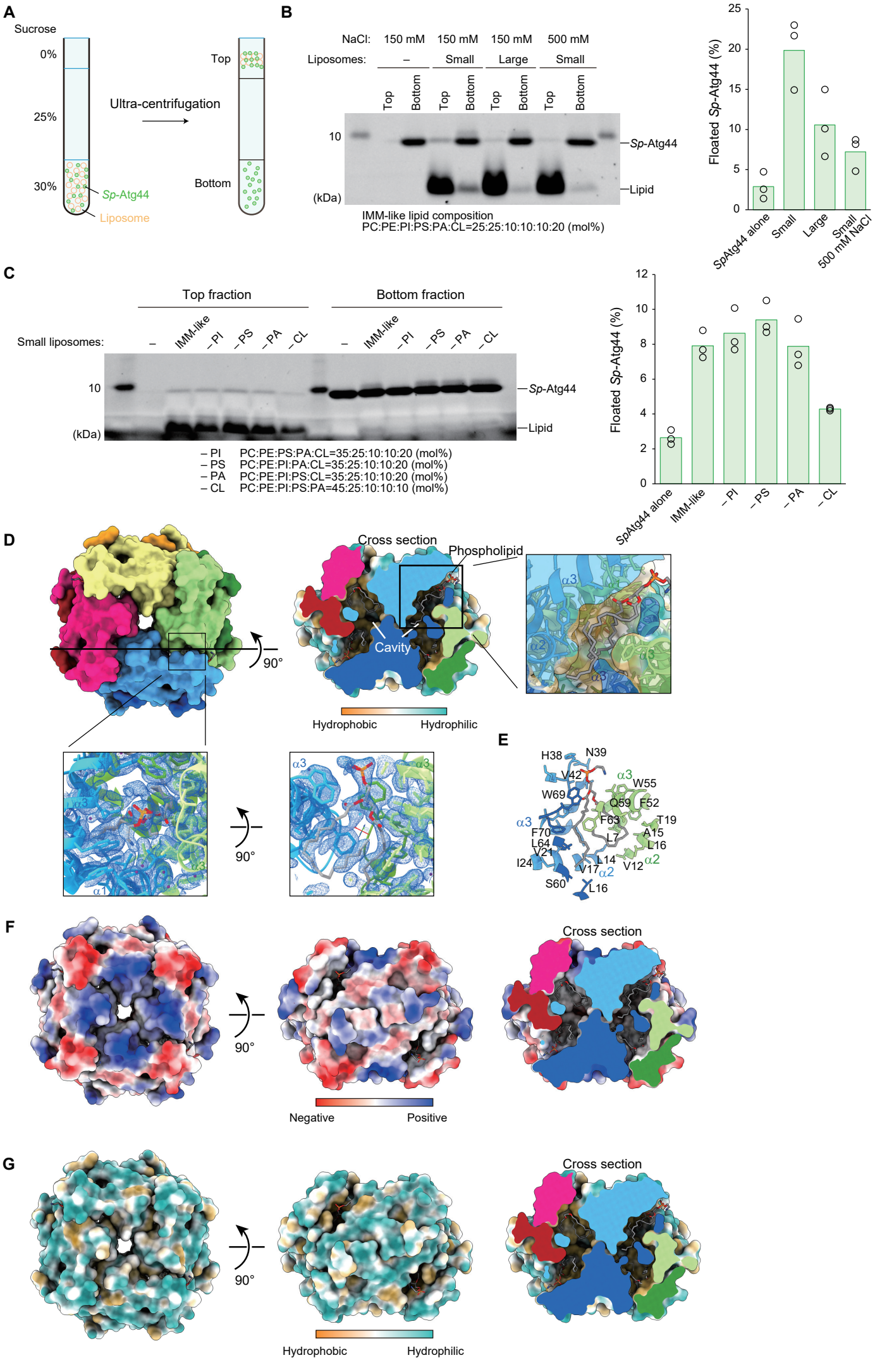
A
Sucrose
0%
25%
30%
Ultra-centrifugation
Top
Bottom
Sp-Atg44
Liposome
B
NaCl: 150 mM 150 mM 150 mM 500 mM
Liposomes: – Small Large Small
Top Bottom Top Bottom Top Bottom Top Bottom
10
(kDa)
Sp-Atg44
Lipid
IMM-like lipid composition
PC:PE:PI:PS:PA:CL=25:25:10:10:10:20 (mol%)
Floated Sp-Atg44 (%)
SpAtg44 alone
Small
Large
Small 500 mM NaCl
C
Top fraction
Bottom fraction
Small liposomes:
– IMM-like – PI – PS – PA – CL
– IMM-like – PI – PS – PA – CL
10
(kDa)
Sp-Atg44
Lipid
– PI PC:PE:PS:PA:CL=35:25:10:10:20 (mol%)
– PS PC:PE:PI:PA:CL=35:25:10:10:20 (mol%)
– PA PC:PE:PI:PS:CL=35:25:10:10:20 (mol%)
– CL PC:PE:PI:PS:PA=45:25:10:10:10 (mol%)
Floated Sp-Atg44 (%)
SpAtg44 alone
IMM-like
– PI
– PS
– PA
– CL
D
90°
Cross section
Phospholipid
Cavity
Hydrophobic
Hydrophilic
α1
α2
α3
90°
E
H38
N39
V42
α3
W55
W69
Q59
F52
F63
T19
α3
F70
L64
V21
L7
A15
L16
I24
L14
V12
α2
V17
α2
S60
L16
F
90°
Cross section
Negative
Positive
G
90°
Cross section
Hydrophobic
Hydrophilic

**Figure S5. Membrane binding and structure of *Sp*-Atg44, related to Figures 5 and 6**

(A) Flotation assay to evaluate the membrane binding of *Sp*-Atg44.

(B) The effect of membrane curvature and electrostatic interaction on the membrane binding of *Sp*-Atg44. The top and bottom fractions in flotation assay were analyzed by SDS-PAGE. Small liposomes were prepared by sonication. Large liposomes were prepared by extrusion through the pore size of 200 nm. The gel was stained with oriole. The ratio of *Sp*-Atg44 in top fraction to total *Sp*-Atg44 (top and bottom) were quantified. Data were mean with plots of three independent experiments.

(C) Lipid selectivity in the membrane binding of *Sp*-Atg44. The top fractions in the flotation assay were analyzed by SDS-PAGE. The gel was stained with oriole. The ratio of *Sp*-Atg44 in top fraction to total *Sp*-Atg44 (top and bottom) were quantified. Data were mean with plots of three independent experiments.

(D) Surface model of *Sp*-Atg44 octamer. Four cavities are organized in the octameric architecture. Two phospholipids are accommodated per cavity. Surface in the cross-section panel is colored according to hydrophilicity. 2Fo-Fc electron density map around a phospholipid modeled as DOPE is shown as blue mesh.

(E) Residues around phospholipid.

(F) Electrostatic potential surface. Negative and positive charges are colored in red and blue, respectively.

(G) Hydrophobicity surface. Hydrophobic and hydrophilic properties are colored in brown and sea green, respectively.

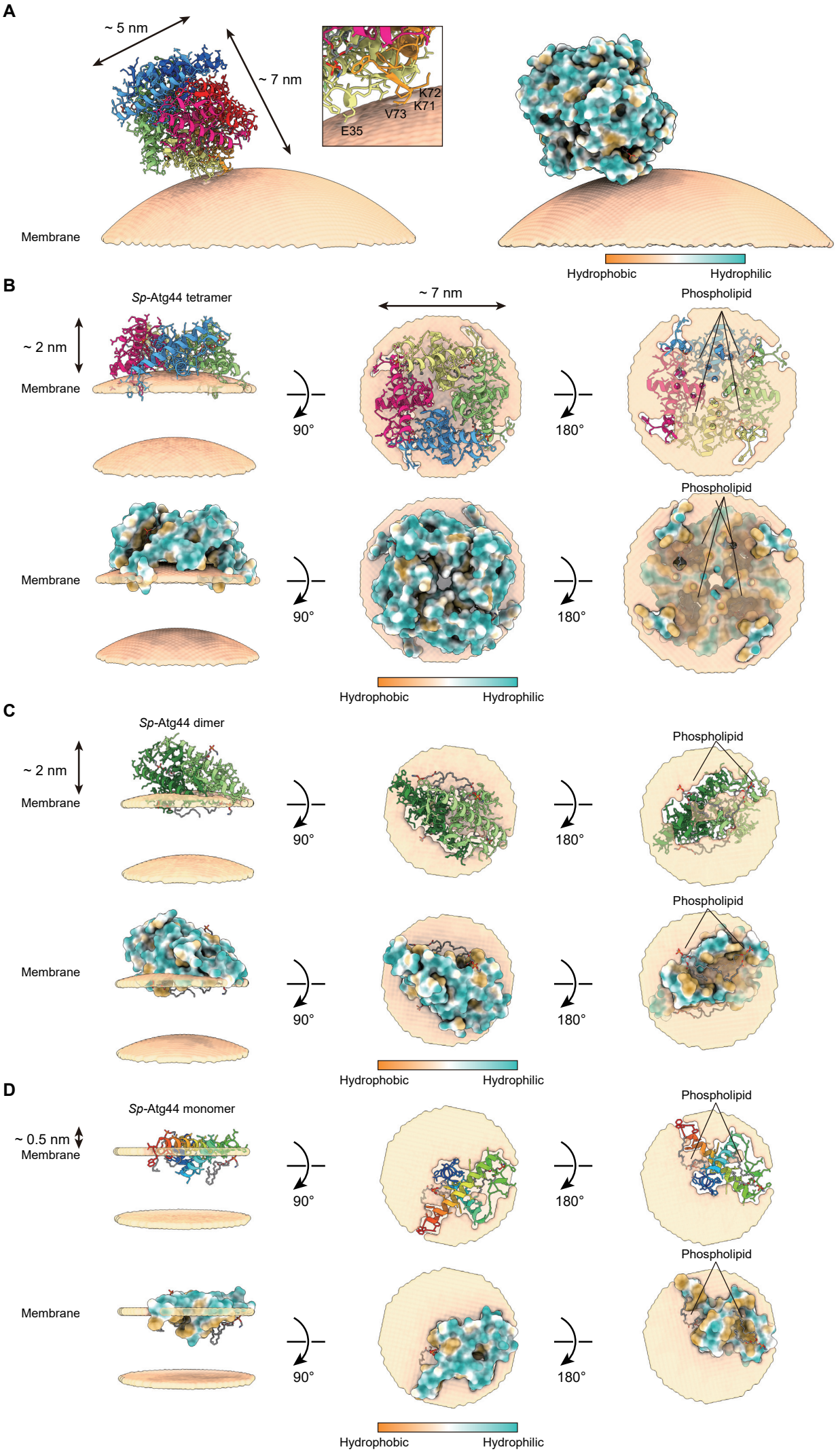
A
~ 5 nm
~ 7 nm
K72
K71
V73
E35
Membrane
Hydrophobic
Hydrophilic
B
Sp-Atg44 tetramer
~ 2 nm
Membrane
~ 7 nm
Phospholipid
90°
180°
Hydrophobic
Hydrophilic
C
Sp-Atg44 dimer
~ 2 nm
Membrane
Phospholipid
90°
180°
Hydrophobic
Hydrophilic
D
Sp-Atg44 monomer
~ 0.5 nm
Membrane
Phospholipid
90°
180°
Hydrophobic
Hydrophilic

**Figure S6. Model of *Sp*-Atg44 on the membrane, related to Figure 6**

(A–D) *Sp*-Atg44 octamer (A), tetramer (B), dimer (C), and monomer (D) on the membrane. The model structures are obtained from the PPM server. The hydrophobic surface of *Sp*-Atg44 is colored according to degree of hydrophobicity or hydrophilicity.

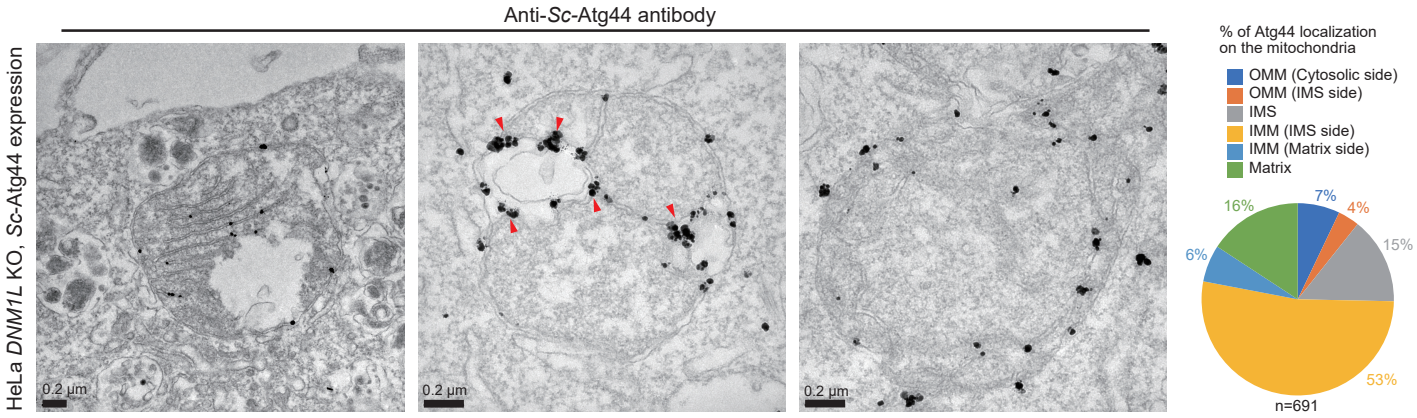


**Figure S7. Atg44 accumulates and exerts its function mainly on the IMM in HeLa cells, related to Figure 7**

*DNM1L*/*Drp1*-knockout HeLa cells were transfected with the *Sc*-Atg44 expression IRES-GFP-NLS vector. The expressed *Sc*-Atg44 was analyzed by immuno-electron microscopy using anti-*Sc*-Atg44 antibody. The localization of *Sc*-Atg44 was classified (on the cytosolic side of the OMM, on the IMS side of the OMM, in the IMS, on the IMS side of the IMM, on the matrix side of the IMM, and in the matrix), and their ratio was quantified. Arrowheads indicate accumulation of *Sc*-Atg44 in IMS. Scale bars and their lengths are provided in each panel.

**Table S1. *S. cerevisiae* strains used in this study, related to STAR★METHODS**

| Strains | Genotype | Source |
|---|---|---|
| BY4742 | *MATα his3Δ1 leu2Δ0 lys2Δ0 ura3Δ0* | (Brachmann et al., 1998)[S1] |
| BY4742 *atg1Δ* | BY4742 *atg1Δ::kanMX* | Horizon |
| SEY6210 | *MATα leu2-3,112 ura3-52 his3-Δ200 trp1-Δ901 suc2-Δ9 lys2-801 GAL* | (Robinson et al., 1988) [S2] |
| TKYM67 | SEY6210 *PEX14-GFP::kanMX* | (Kanki and Klionsky, 2008)[S3] |
| TKYM72 | SEY6210 *PEX14-GFP::kanMX atg1Δ::HIS3* | (Kanki and Klionsky, 2008)[S3] |
| TKYM236 | SEY6210 *pho8Δ60::HIS3 pho13Δ::LEU2* | (Aoki et al., 2011)[S4] |
| TKYM256 | SEY6210 *pho8Δ60::HIS3 pho13Δ::LEU2 atg1Δ::URA3* | (Aoki et al., 2011)[S4] |
| TKYM307 | SEY6210 *IDH1-GFP::TRP1* | (Furukawa et al., 2018)[S5] |
| TKYM365 | SEY6210 *GFP-ATG8::LEU2* | (Furukawa et al., 2018)[S5] |
| TKYM502 | SEY6210 *IDH1-GFP::TRP1* | This study |
| TKYM513 | SEY6210 *IDH1-GFP::TRP1 atg44Δ::HIS3* | This study |
| TKYM566 | SEY6210 *atg44Δ::kanMX MIA40-GFP::natNT* | This study |
| TKYM586 | SEY6210 *IDH1-GFP::TRP1 fzo1Δ::LEU2* | This study |
| TKYM588 | SEY6210 *IDH1-GFP::TRP1 atg44Δ::HIS3 fzo1Δ::LEU2* | This study |
| TKYM590 | SEY6210 *IDH1-GFP::TRP1 atg44Δ::kanMX mgm1Δ::HIS3* | This study |
| TKYM593 | SEY6210 *IDH1-GFP::TRP1 mgm1Δ::HIS3* | This study |
| TKYM614 | SEY6210 *OM14-RFP::HIS3 atg44Δ::kanMX* | This study |
| TKYM616 | SEY6210 *OM14-mCherry::kanMX* | This study |
| TKYM626 | SEY6210 *atg44Δ::kanMX OM14-mCherry::hphNT* | This study |
| TKYM630 | SEY6210 *dnm1Δ::kanMX OM14-mCherry::hphNT* | This study |
| YKF28 | SEY6210 *IDH1-GFP::TRP1 atg1Δ::HIS3* | (Furukawa et al., 2018)[S5] |
| YKF82 | SEY6210 *GFP-ATG8::LEU2 atg1Δ::kanMX* | (Furukawa et al., 2018)[S5] |
| YKF91 | SEY6210 *atg44Δ::kanMX* | This study |
| YKF92 | SEY6210 *IDH1-GFP::TRP1 atg44Δ::kanMX* | This study |

| | | |
|---|---|---|
| YKF95 | SEY6210 *pho8Δ60::HIS3 pho13Δ::LEU2 atg44Δ::kanMX* | This study |
| YKF97 | SEY6210 *PEX14-GFP::kanMX atg44Δ::HIS3* | This study |
| YKF100 | BY4742 *IDH1-GFP::HIS3 ypt7Δ::LEU2* | (Yamashita et al., 2016)[S6] |
| YKF143 | SEY6210 *SEC63-GFP::TRP1* | This study |
| YKF148 | SEY6210 *SEC63-GFP::TRP1 atg1Δ::kanMX* | This study |
| YKF156 | SEY6210 *atg11Δ::LEU2 atg32Δ::HIS3 atg44Δ::kanMX* | This study |
| YKF247 | SEY6210 *GFP-ATG8::LEU2 atg44Δ::kanMX* | This study |
| YKF249 | SEY6210 *SEC63-GFP::TRP1 atg44Δ::kanMX* | This study |
| YKF250 | BY4742 *IDH1-GFP::hphNT* | This study |
| YKF251 | BY4742 *IDH1-GFP::hphNT atg44Δ::kanMX* | This study |
| YKF252 | BY4742 *IDH1-GFP::hphNT mgm1Δ::kanMX* | This study |
| YKF253 | BY4742 *IDH1-GFP::hphNT dnm1Δ::kanMX* | This study |
| YKF254 | BY4742 *IDH1-GFP::hphNT dnm1Δ::kanMX mgm1Δ::HIS3* | This study |
| YKF255 | BY4742 *IDH1-GFP::hphNT atg44Δ::kanMX mgm1Δ::HIS3* | This study |
| YKF258 | BY4742 *IDH1-GFP::HIS3 ypt7Δ::LEU2 atg44Δ::kanMX* | This study |
| YKF259 | BY4742 *OM45-GFP::HIS3 ypt7Δ::LEU2 atg44Δ::kanMX* | This study |
| YKF269 | BY4742 *IDH1-GFP::hphNT atg44Δ::kanMX atg1Δ::natNT* | This study |
| YKF270 | BY4742 *IDH1-GFP::hphNT atg44Δ::kanMX atg8Δ::natNT* | This study |
| YKF271 | BY4742 *IDH1-GFP::hphNT atg44Δ::kanMX atg11Δ::natNT* | This study |
| YKF272 | BY4742 *IDH1-GFP::hphNT atg44Δ::kanMX atg32Δ::natNT* | This study |
| YKF276 | BY4742 *atg44Δ::kanMX* | This study |
| YKF289 | BY4742 *natNT::CUP1p-GFP-ATG32* | This study |
| YKF290 | BY4742 *atg44Δ::kanMX natNT::CUP1p-GFP-ATG32* | This study |
| YKF291 | BY4742 *atg44Δ::kanMX OM14-RFP-HIS natNT::CUP1p-GFP-ATG32* | This study |
| YKF292 | BY4742 *atg44Δ::kanMX OM14-RFP-HIS natNT::CUP1p-GFP-ATG8* | This study |
| YKF293 | BY4742 *atg44Δ::kanMX OM14-RFP-HIS natNT::CUP1p-GFP-ATG11* | This study |
| YKYM30 | SEY6210 *atg11Δ::LEU2 atg32Δ::HIS3* | (Furukawa et al., 2018)[S5] |

**Table S2. *S. pombe* strains used in this study, related to STAR★METHODS**

| Strains | Genotype | Source |
|---|---|---|
| 972 | *h-* | Laboratory stock |
| TFSP407 | *h- ura4-D18 tuf1-mRFP::ura4* | (Fukuda et al., 2020)[S7] |
| TFSP519 | *h- yop1-mEGFP::kan* | This study |
| TFSP523 | *h- yop1-mEGFP::kan atg1Δ::nat* | This study |
| TFSP667 | *h- ura4-D18 tdh1-mRFP::ura4 sdh2-mEGFP::nat* | This study |
| TFSP669 | *h- ura4-D18 tuf1-mRFP::ura4 sdh2-mEGFP::nat* | (Fukuda et al., 2020)[S7] |
| TFSP743 | *h- pgk1-mEGFP::hph* | (Fukuda et al., 2020)[S7] |
| TFSP785 | *h- pgk1-mEGFP::kan atg1Δ::nat* | This study |
| TFSP1001 | *h- ura4-D18 tdh1-mRFP::ura4 sdh2-mEGFP::nat atg44Δ::kanMX4* | This study |
| TFSP1005 | *h- pgk1-mEGFP::hph atg44Δ::kanMX4* | This study |
| TFSP1031 | *h- yop1-mEGFP::kan atg44Δ::nat* | This study |
| TFSP1085 | *h- ura4-D18 tuf1-mRFP::ura4 atg44Δ::kanMX4* | This study |
| TFSP1209 | *h- ura4-D18 tuf1-mRFP::ura4 sdh2-mEGFP::nat dnm1Δ::hph* | This study |
| TFSP1213 | *h- ura4-D18 tuf1-mRFP::ura4 dnm1Δ::nat* | This study |
| TFSP1217 | *h- ura4-D18 tuf1-mRFP::ura4 atg44Δ::kanMX4 dnm1Δ::nat* | This study |
| TFSP1277 | *h- ura4-D18 tuf1-mRFP::ura4 sdh2-mEGFP::nat mgm1Δ::hph* | This study |
| TFSP1283 | *h- ura4-D18 tuf1-mRFP::ura4 sdh2-mEGFP::nat atg44Δ::kanMX4 mgm1Δ::hph* | This study |
| TFSP1345 | *h- ura4-D18 tuf1-mRFP::ura4 sdh2-mEGFP::nat dnm1Δ::hph msp1Δ::kan* | This study |
| TFSP1391 | *h- ura4-D18 tuf1-mRFP::ura4 sdh2-mEGFP::nat hph::P3nmt1:atg44* | This study |
| TFSP1485 | *h- ura4-D18 tuf1-mRFP::ura4 sdh2-mEGFP::nat dnm1Δ::hph kan::P3nmt1:atg44* | This study |
| TFSP3177 | *h- tom70-mEGFP::hph mic60-FLAG::kan tuf1-mRFP::nat* | This study |
| TFSP3331 | *h- ura4-D18 tuf1-mRFP::ura4 atg44Δ::hph* | This study |
| TFSP3833 | *h- ura4-D18 tuf1-mRFP::ura4 sdh2-mEGFP::nat atg44Δ::kanMX4* | This study |

| | | |
|---|---|---|
| TFSP4541 | *h- ura4-D18 tdh1-mRFP::ura4 sdh2-mEGFP::nat atg1Δ::hph* | This study |
| TFSP4563 | *h- ura4-D18 tuf1-mRFP::ura4 sdh2-mEGFP::nat atg1Δ::nat* | This study |

SUPPLEMENTAL REFERENCES


S1. Brachmann, C.B., Davies, A., Cost, G.J., Caputo, E., Li, J., Hieter, P., and Boeke, J.D. (1998). Designer deletion strains derived from Saccharomyces cerevisiae S288C: a useful set of strains and plasmids for PCR-mediated gene disruption and other applications. Yeast *14*, 115-132. 10.1002/(SICI)1097-0061(19980130)14:2<115::AID-YEA204>3.0.CO;2-2.

S2. Robinson, J.S., Klionsky, D.J., Banta, L.M., and Emr, S.D. (1988). Protein sorting in Saccharomyces cerevisiae: isolation of mutants defective in the delivery and processing of multiple vacuolar hydrolases. Mol. Cell. Biol. *8*, 4936-4948. 10.1128/mcb.8.11.4936-4948.1988.

S3. Kanki, T., and Klionsky, D.J. (2008). Mitophagy in yeast occurs through a selective mechanism. J. Biol. Chem. *283*, 32386-32393. 10.1074/jbc.M802403200.

S4. Aoki, Y., Kanki, T., Hirota, Y., Kurihara, Y., Saigusa, T., Uchiumi, T., and Kang, D. (2011). Phosphorylation of Serine 114 on Atg32 mediates mitophagy. Mol. Biol. Cell *22*, 3206-3217. 10.1091/mbc.E11-02-0145.

S5. Furukawa, K., Fukuda, T., Yamashita, S.I., Saigusa, T., Kurihara, Y., Yoshida, Y., Kirisako, H., Nakatogawa, H., and Kanki, T. (2018). The PP2A-like Protein Phosphatase Ppg1 and the Far Complex Cooperatively Counteract CK2-Mediated Phosphorylation of Atg32 to Inhibit Mitophagy. Cell Rep. *23*, 3579-3590. 10.1016/j.celrep.2018.05.064.

S6. Yamashita, S.I., Jin, X., Furukawa, K., Hamasaki, M., Nezu, A., Otera, H., Saigusa, T., Yoshimori, T., Sakai, Y., Mihara, K., and Kanki, T. (2016). Mitochondrial division occurs concurrently with autophagosome formation but independently of Drp1 during mitophagy. J. Cell Biol. *215*, 649-665. 10.1083/jcb.201605093.

S7. Fukuda, T., Ebi, Y., Saigusa, T., Furukawa, K., Yamashita, S.I., Inoue, K., Kobayashi, D., Yoshida, Y., and Kanki, T. (2020). Atg43 tethers isolation membranes to mitochondria to promote starvation-induced mitophagy in fission yeast. eLife *9*. 10.7554/eLife.61245.